MOLECULAR IMAGING AND BIOLOGY
© Academy of Molecular Imaging 2005
Published Online: 2 December 2005

Mol Imaging Biol (2006) 8:1–8
DOI: 10.1007/s11307-005-0027-y

ORIGINAL ARTICLE

Synthesis and Positron Emission Tomography Evaluation of Three Norepinephrine Transporter Radioligands: [C-11]Desipramine, [C-11]Talopram and [C-11]Talsupram

Magnus Schou, MSc,[1,2] Judit Sóvágó, MD,[1] Victor W. Pike, PhD,[2] Balázs Gulyás, MD, PhD,[1] Klaus P. Bøgesø, PhD,[3] Lars Farde, MD, PhD,[1] Christer Halldin, PhD[1]

[1]*Karolinska Institutet, Department of Clinical Neuroscience, Psychiatry Section, Karolinska Hospital, S-17176 Stockholm, Sweden*
[2]*Molecular Imaging Branch, National Institute of Mental Health, National Institutes of Health, Building 10 Rm. B3 C346A, 10 Center Drive, Bethesda, MD 20892-1003, USA*
[3]*H. Lundbeck A/S, Copenhagen, Denmark*

Abstract

Desipramine (DMI), talopram and talsupram, three of the most potent norepinephrine transporter (NET) inhibitors reported to date, were radiolabeled in high yields and at high specific radioactivity (58–75 GBq/μmol) by the methylation of nor-precursors with [C-11]methyl triflate. The regional brain distribution of each radioligand following intravenous injection into cynomolgus monkey was examined *in vivo* with positron emission tomography (PET). For all three radioligands, the regional brain distribution of radioactivity was slightly heterogeneous, with higher uptake of radioactivity in the mesencephalon, thalamus and lower brainstem than in striatum. The rank order of maximal brain radioactivity (as percentage of injected dose) was [C-11]DMI (2.7%) > [C-11]talsupram (1.3%) > [C-11]talopram (0.7%). The appearance of radioactive metabolites in plasma was similar for each radioligand (75–85% of radioactivity in plasma at 45 min). These metabolites were all more polar than their parent radioligand. The data show that these radioligands are inferior to existing radioligands for the study of brain NET with PET *in vivo*.

Key words: Norepinephrine transporter, PET, Desipramine, Talopram, Talsupram

Introduction

Most research on the development of radioligands for imaging the major brain monoamine transporters with positron emission tomography (PET) has so far been directed towards the dopaminergic and serotonergic transporters (DAT and SERT, respectively) [1]. By contrast compounds that have been labelled and evaluated as PET radioligands for brain norepinephrine transporters (NETs) are so far very few, but include [C-11]nisoxetine [2], and two analogs of reboxetine, known as (*S,S*)-[C-11]MeNER [3–5] and (*S,S*)-[F-18]FMeNER-D_2 (Fig. 1) [6]. Only the reboxetine analogs are able to image NET with PET, but as it appears not with high sensitivity.

In view of our aim to develop a PET radioligand that is suitable for the sensitive and quantitative measurement of NET in the human brain, we are interested in evaluating selective and high affinity NET inhibitors from various structural classes. Desipramine (DMI), talopram and talsupram (Fig. 1) are effective antidepressants [7, 8] and are three of the most potent and selective inhibitors of NET

Correspondence to: Magnus Schou, MSc; *e-mail:* magnus.schou@cns.ki.se

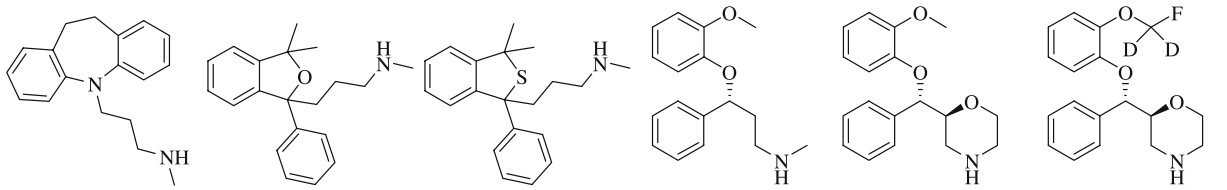

Fig. 1. Structures and properties of NET inhibitors. It should be noted that the data was obtained from different sources and is thus not entirely comparable.

reported to date (Table 1) [9]. As such, we were led to consider these compounds as potential radioligands for imaging NET with PET.

DMI, is a classical tricyclic antidepressant that has some anticholinergic properties. However, DMI binding to NET is selective and of high affinity. Thus, its binding to human NET (Ki = 0.63 nM) [11] is about 100-fold higher than its affinity towards muscarinic acetylcholinergic receptors (Ki = 66 nM) [10]. Furthermore, DMI affinity for rat NET is over 216-fold greater than that towards SERT and 9381-fold greater than that towards DAT [9]. Tritium-labelled DMI has been used for *in vitro* autoradiographic studies of NET in the human brain *post mortem* [12, 13]. From one of these studies, it was concluded that [H-3]DMI bound to high- and low-affinity binding sites, where the high affinity portion of the binding was considered to be NET-specific [12]. Although [C-11]DMI has been synthesized previously [14], no data on its brain distribution *in vivo* have been reported.

Talopram and talsupram are bicyclic phenylphthalans that are very closely related in structure to each other, differing only in the nature of one heterocyclic atom (O or S, respectively), and are also structurally similar to the selective and high affinity SERT inhibitor, citalopram [7, 8]. Inhibition constants for monoamine uptake into rat hypothalamic synaptosomes [8] for these compounds are in the nanomolar range (Table 1). Talopram and talsupram are highly selective for NET *versus* DAT and SERT (Table 1) and are over 100-fold selective for NET *versus* all other targets that they have been tested against (K.P. Bøgesø, personal communication).

Table 1. IC_{50} values for inhibition of [^{3}H]monoamine uptake into rat brain synaptosomes

IC_{50} (nM)			
Ligand	SERT	NET	DAT
DMI	210	0.97	9100
Talopram	1400	2.9	44000
Talsupram	850	0.79	9300

Concurrent with this study, McConathy et al. reported an evaluation of [C-11]talopram and [C-11]talsupram as radioligands in rhesus monkeys *in vivo* [15]. Their report showed that the global brain radioactivity uptake was low for each radioligand, but did not cover brain regional differences in uptake. Several factors may lead to low brain uptake of candidate radioligands, including, for example, high binding to plasma proteins, rapid metabolism, rapid clearance from plasma or rapid removal from brain by efflux pumps. These effects may in certain cases be species-dependent.

This report provides an evaluation of [C-11]DMI as a radioligand for brain NET in cynomolgus monkey and extends the findings of McConathy et al. [15] on [C-11]talopram and [C-11]talsupram in a different species of monkey at a brain regional level.

Materials and Methods

Chemistry

General Procedures. DMI was obtained from Sigma. Nor-precursors and authentic talopram and talsupram (racemates) were kindly supplied by H. Lundbeck A/S (Copenhagen, Denmark). Other chemicals were obtained from Sigma-Aldrich and used without further purification. Nor-DMI was synthesized according to a previously described method [14]. [C-11]Carbon dioxide was produced at the Karolinska Hospital with a GEMS PETtrace cyclotron using 16 MeV protons in the N-14(p,α) C-11 reaction on nitrogen gas. [C-11]Methyl iodide was synthesized from [C-11]carbon dioxide with a GEMS PETtrace MeI Microlab® apparatus [16]. [C-11]Methyl triflate was prepared by sweeping [C-11]methyl iodide vapour through a heated glass column containing silver-triflate-impregnated graphitized carbon, as previously described [16].

Preparative HPLC was performed using a reverse phase μ-Bondapak C-18 column (300 × 7.8 mm, 10 μm; Waters) or a normal phase μ-Porasil column (300 × 7.8 mm; Waters). The column outlets were connected to an absorbance detector (λ = 254 nm) in series with a GM tube for radiation detection. [C-11]DMI was purified by normal phase HPLC with system A (CH_2Cl_2–MeOH–TEA; 99: 1: 0.01 by vol.) as mobile phase at 2 ml/min. [C-11]talopram and [C-11]talsupram were purified using reverse

phase HPLC on system B (MeCN–NH_4CO_2H (0.1 M); 40: 60 v/v) eluted at 6 ml/min and 8 ml/min, respectively.

The radiochemical purity of each product was determined by reverse phase HPLC equipped with a μ-Bondapak C-18 column (300 × 3.9 mm, 10 μm; Waters) and an absorbance detector (λ = 254 nm) in series with a β-flow detector (Beckman) for radiation detection. [C-11]DMI and [C-11]talsupram were analysed using mobile phase C (MeCN-H_3PO_4 (10 mM), 35: 65 v/v) at 3 ml/min. [C-11]Talopram was analysed using mobile phase D (MeCN-H_3PO_4 (10 mM), 30: 70 v/v) at 3 ml/min.

Radiomethylation Procedure. [C-11]Methyl triflate was trapped at room temperature in a reaction vessel containing the appropriate nor-precursor of DMI, talopram or talsupram (0.5 mg; 2, 1.8 or 1.7 μmol, respectively) and aqueous sodium hydroxide solution (0.5 M; 2, 6 or 6 μl, respectively) in acetone (400 μl) (Scheme 1). After completed trapping, mobile phase (system A or B, 600 μl) was added to the crude reaction mixture before its injection onto the semi-preparative HPLC column. The mobile phase was evaporated off from the collected radioactive product fraction and the residue dissolved in sterile sodium phosphate buffered saline (pH 7.4; 8 ml) and filtered through a sterile Millipore filter (0.22 μm), yielding the product in a sterile solution free from pyrogens.

PET Measurements

A Siemens ECAT EXACT HR PET system was run in 3-D mode. The spatial resolution is about 3.8 mm FWHM. Images were displayed as 47 sections with a separation of 3.3 mm [17].

Two cynomolgus monkeys (5.65 and 6.31 kg) were supplied by the National Institute for Infectious Disease Control (Solna, Stockholm). The study was approved by the Animal Ethics Committee of Northern Stockholm. Anaesthesia was induced and maintained by repeated intramuscular injection of a mixture of ketamine (3–4 mg $kg^{-1}h^{-1}$ Ketalar®, Parke-Davis) and xylazine hydrochloride (1–2 mg $kg^{-1}h^{-1}$ Rompun® vet., Bayer Sweden). A fixation system was used to secure a position of the monkey head during the PET measurements [18]. Body temperature was controlled by a heating pad with thermostat. In each PET measurement 49–55 MBq of radioligand was injected as a bolus into the left sural vein. Radioactivity in brain was measured according to a pre-programmed sequence of frames over 93 minutes.

In the first monkey, a baseline measurement with [C-11]DMI (53 MBq; 65 GBq/μmol) was performed followed by a pre-treatment measurement in which DMI (5 mg/kg) was injected intravenously 20 minutes before injection of [C-11]DMI (50 MBq; 52 GBq/μmol). Both PET measurements were performed on the same day.

In the second monkey, two baseline PET measurements were performed on the same day, the first with [C-11]talopram (55 MBq; 58 GBq/μmol) and the second with [C-11]talsupram (49 MBq; 75 GBq/μmol).

Regions of interest (ROI's) (lower brainstem, mesencephalon, striatum, thalamus and whole brain) were drawn on images reconstructed as a sum of all frames and were defined according to an atlas of a cryosected Cynomolgus monkey head *in situ* [18]. Radioactivity was calculated for the sequence of time-frames, corrected for the radioactivity decay and plotted *versus* time. The percent of injected radioactivity present in brain at the time of maximal radioactivity concentration was used as an index of radioligand uptake in the brain. This percentage was calculated by multiplying the brain volume (about 70 ml) with the radioactivity concentration in the ROI for the whole brain divided by the injected radioactivity. The brain volume was calculated by multiplying the sum of the whole brain regions of all PET-sections with the plane separation.

Striatum, which is a region almost devoid of NETs [19–21], was used as a reference region for the free radioligand concentration and non-specific binding in brain. To calculate specific binding, radioactivity in the striatum was subtracted from the radioactivity in a ROI.

Analysis of Radioactive Metabolites in Plasma

A HPLC method was used to determine the percentages of radioactivity in monkey plasma that correspond to unchanged radioligand and labelled metabolites during the course of a PET measurement. The method was adapted from that known to be useful for other PET radioligands [22]. Venous blood samples (2 ml) were obtained from the monkey at 4, 15, 30 and 45 minutes after injection of radioligand. Plasma (0.5 ml), obtained after centrifugation at 2,000 g for two minutes, was mixed with

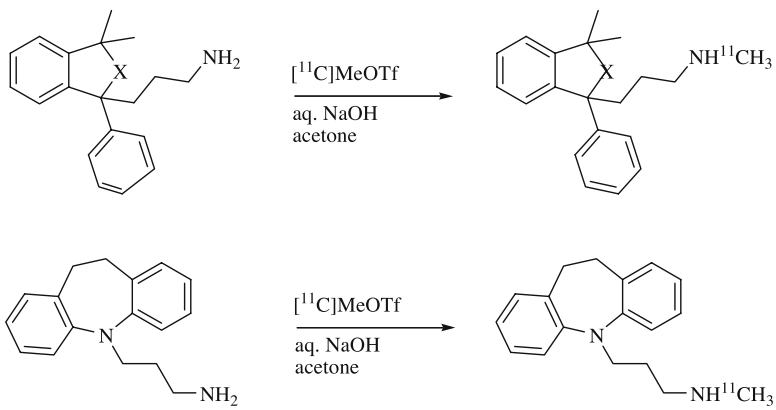

Scheme 1. Labelling of [C-11]DMI, [C-11]talopram (*X* = *O*) and [C-11]talsupram (*X* = *S*).

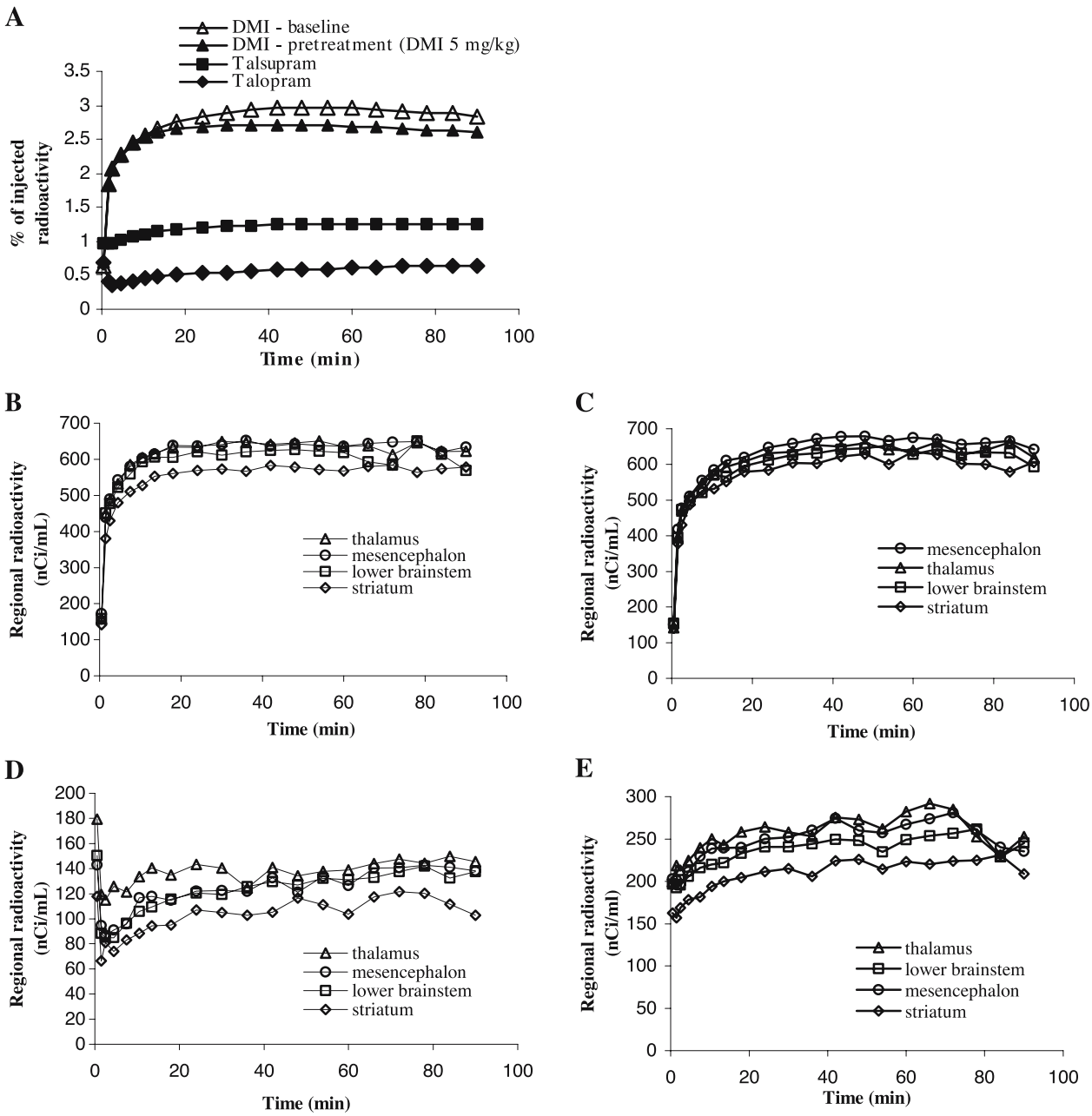

Fig. 2. (**A**) Whole brain radioactivity as percentage of injected radioactivity of the radioligands [C-11]DMI, [C-11]talopram and [C-11]talsupram. (**B**) Time–radioactivity curve obtained after i.v. injection of [C-11]DMI showing regional brain distribution under baseline conditions. (**C**) Regional brain distribution of [C-11]DMI under pre-treatment conditions. (**D**) Time–radioactivity curve obtained after i.v. injection of [C-11]talopram. (**E**) Time–radioactivity curve obtained after i.v. injection of [C-11]talsupram. The injected radioactivity was normalized to 50 MBq in Fig. 2B–E.

acetonitrile (0.7 ml). The supernatant acetonitrile-plasma mixture (1.1 ml) and the precipitate obtained after centrifugation at 2,000 g for 2 minutes were counted in a NaI well-counter.

The HPLC system used in the experiments consisted of an interface module (D-7000; Hitachi), a L-7100 pump (Hitachi), an injector (model 7125 with a 1.0 ml loop; Rheodyne) equipped with a μ-Bondapak-C18 column (300 × 7.8 mm, 10 μm; Waters) and an absorbance detector (L-7400; 254 nm; Hitachi) in series with a radiation detector (Radiomatic 150TR; Packard) equipped with a PET Flow Cell (600 μl cell). Phosphoric acid (10 mM) (E) and acetonitrile (F) were used as the mobile phase at 6.0 ml/min, according to the following program: 0–5.5 min, (E: F) 90: 10 v/v − 40: 60 v/v; 5.5–6.5 minutes, (E: F) 40: 60–90 v/v: 10; 6.5–10 minutes (E: F) 90: 10 v/v. The radioactive compound having a retention time

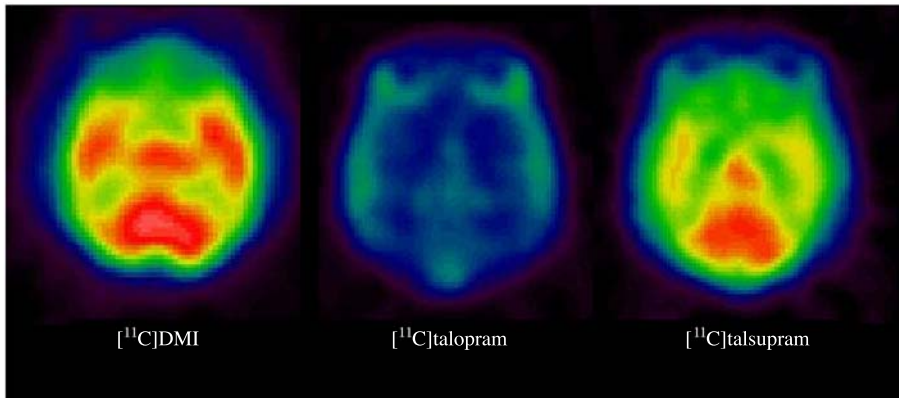

Fig. 3. Horizontal PET images showing the level of mesencephalon and cortex after i.v. injection of [C-11]DMI, [C-11]talopram and [C-11]talsupram. The intensity scale is different on the three PET images. The [C-11]DMI image scale is from 0 to 750 nCi/ml, whereas the PET images obtained after i.v. injection of [C-11]talopram and [C-11]talsupram are scaled from 0 to 325 nCi/ml.

corresponding to reference NET inhibitor (DMI, talopram or talsupram) was integrated and its area expressed as a percentage of the sum of the areas of all detected radioactive compounds (decay-corrected).

Results

Radiochemistry

The radiochemical yield (decay-corrected) of each radioligand from [C-11]methyl triflate was high (~60%, assessed by using radio-HPLC). The total radiosynthesis time was 30–35 min and the radiochemical purities were higher than 99%. The retention times (t_R's) of [C-11]DMI, [C-11]talopram and [C-11]talsupram in the preparative HPLC systems were 8.5, seven and 10 minutes, respectively. The t_R's of DMI, talopram and talsupram in the analytical HPLC systems were 4, 6.5 and 6 minutes, respectively. The specific radioactivities at the times of injection into monkey were 58–75 GBq/μmol.

PET Measurements

After intravenous administration of [C-11]DMI, radioactivity readily entered brain reaching a peak of 2.7% of the injected dose at 24 minutes after injection (Fig. 2A). No ratio of radioactivity greater than 1.15 was found between any ROI and striatum over the time course of the experiment (Fig. 2B). A higher uptake of radioactivity in brain was obtained in the pretreatment experiment (3.0%), though DMI had no significant effect on the brain distribution of radioactivity (Fig. 2C). PET images of cynomolgus monkey brain, obtained at nine to 93 minutes after [C-11]DMI injection reflect the adequate uptake of radioactivity and the lack of a regional distribution of this radioactivity according to the expected distribution of NET (Fig. 3, Panel A).

Following intravenous injection of [C-11]talopram or [C-11]talsupram, maximal brain uptake of radioactivity was 0.7% or 1.2% of the injected dose, respectively (Fig. 2A). For each radioligand, the highest uptake of radioactivity was observed in the lower brainstem, mesencephalon and thalamus, whereas radioactivity was lowest in striatum (Fig. 2D and E). The peak ratios of radioactivity in thalamus to that in striatum were 1.3 for [C-11]talopram at 66 min and 1.4 for [C-11]talsupram at 90 minutes. For each radioligand, The PET images of cynomolgus brain, obtained at 9 to 93 minutes after [C-11]talopram injection reflects the very low uptake of radioactivity (Fig. 3, Panel A), while the corresponding image for [C-11]talopram reflects a higher uptake of radioactivity with a more discrete distribution (Fig. 3, Panel B).

Analysis of Radioactive Metabolites in Plasma

The radioactivity in monkey plasma corresponding to unchanged [C-11]DMI was 60% at 30 minutes and 20% at

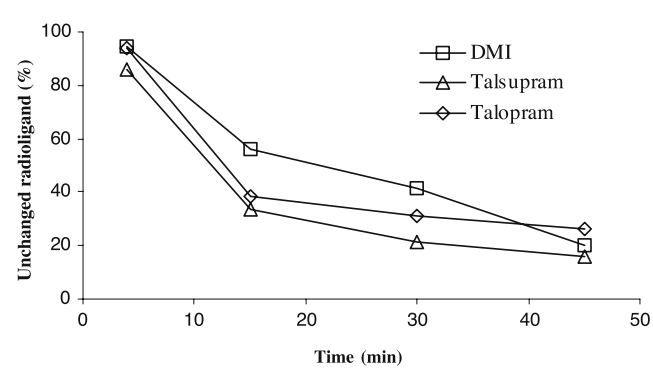

Fig. 4. Percentage of unchanged radioligand at 4, 15, 30 and 45 minutes after i.v. injection of [C-11]DMI, [C-11]talopram and [C-11]talsupram.

45 minutes after injection (Fig. 4). For [C-11]talopram the corresponding values were 30% at 30 min and 25% at 45 minutes, and for [C-11]talsupram 20% at 30 minutes and 15% at 45 minutes. Radioactive metabolites of [C-11]DMI, [C-11]talopram and [C-11]talsupram were all less lipophilic than the parent compound, as judged by their shorter retention times in the reverse phase HPLC analysis.

Discussion

Brain uptake of radioactivity after intravenous administration of [C-11]DMI to cynomolgus monkey was satisfactory for a candidate PET radioligand (Fig. 2, Panel A). However, the regional brain distribution of radioactivity was almost completely homogeneous, as shown in the regional time-activity curves (Fig. 2, Panel B) and in the acquired PET image (Fig. 3, Panel A). The ratio between any NET-rich region, such as thalamus, and the NET-poor striatum did not exceed 1.15 during the baseline experiment. The distribution of radioactivity was insensitive to pre-treatment with DMI (Fig. 2, Panel C). These findings contrast with results from the *in vitro* autoradiography of [H-3]DMI binding to human brain *post mortem* where most of the binding was inhibited by DMI [12, 13]. The difference between the results *in vivo* and *in vitro* may be due to species differences and/or the washing steps that may only be utilized *in vitro* but which may effectively remove non-specific binding.

The increased uptake of radioactivity into brain after pre-treatment with DMI indicates that the plasma-free concentration of radioligand is sensitive to DMI pre-treatment, probably due to inhibition of DMI binding in the periphery. This accords with the results obtained with (*S,S*)-[C-11]MeNER, which showed increased brain radioactivity in cynomolgus monkey after intravenous pre-treatment with DMI [3]. However, it should be noted that since DMI was used in the pre-treatment, peripheral blockade might not be limited to NET but may include other unknown DMI-binding sites.

The percentages of [C-11]talopram or [C-11]talsupram that maximally entered cynomolgus brain were low (0.7% and 1.2% of injected dose, respectively) and similar to those that have been observed in rhesus monkey (~0.07% of injected dose per g) [15]. The shapes of the global brain radioactivity uptake curves for the two radioligands were similar to each other in this study and also to those in rhesus monkey reported by McConathy et al. [15]. After the initial low uptake of radioactivity into brain, there was only a slight increase over the remainder of the experiment (Fig. 2, Panel A) The low brain uptake may be due, at least in part, to the high degrees of protonation and low overall lipohilicities of these ligands (ionized plus unionized species) at physiological pH. Thus, the calculated *pKa* values are 10.4 and 10.5, for talopram and talsupram, respectively, while the calculated Log*D* values [23] (at pH 7.4) are 1.02 and 1.60 [24] and similar to the empirical Log*D* values of 0.8 and 1.7, respectively (Fig. 1) [15]. Notably, talsupram has a slightly higher Log*D* value than talopram and has the higher brain penetration. However, [C-11]DMI has a low *c*Log*D* value (0.91; Fig. 1) comparable to that of [C-11]talopram but still achieves acceptable brain entry (Fig. 2, Panel A). Other radioligands with low Log*D* values are know to enter brain adequately for PET imaging (e.g., [C-11]raclopride; cLog*D* = 0.7) [24]. Hence, effects other than low logD may also be operating to reduce the brain entry of [C-11]talopram and [C-11]talsupram. Possible mechanisms for the low brain uptake of these two radioligands include strong binding to plasma proteins or removal from brain by efflux pumps, such as Pgp. These possibilities were not investigated further, because at present there are no practical means for overcoming such effects in clinical studies.[1]

Although after intravenous administration of either [C-11]talopram or [C-11]talsopram into cynomolgus monkey the proportion of radioactivity entering brain was low, small regional differences in brain radioactivity were indeed observed (Fig. 2, Panels D and E), whereas McConathy et al. [15] did not detect such differences in rhesus monkey. Ratios of radioactivity in thalamus to striatum reached 1.3 and 1.4 for [C-11]talopram and [C-11]talsupram, respectively. These values are higher than for [C-11]DMI, but somewhat less than the corresponding values in earlier imaging studies with (*S,S*)-[C-11]MeNER and (*S,S*)-[F-18]FMeNER-D_2 where ratios of about 1.5 were obtained in cynomolgus monkeys [3, 6] and baboons [5]. A ratio of about 2.5 was also obtained with (*S,S*)-[C-11]MeNER in rodent brain [4].

In this study, the same protocol used in our previous studies with (*S,S*)-[C-11]MeNER and (*S,S*)-[F-18]FMeNER-D_2 was used to induce and maintain anaesthesia throughout the PET experiment. Although one of the anaesthetic agents used, ketamine, is known to bind to NET [27, 28], (*S,S*)-[C-11]MeNER and (*S,S*)-[F-18]FMeNER-D_2 readily entered brain and accumulated in NET-rich regions under these anaesthetic conditions [5, 6]. It therefore seems unlikely that ketamine influences the global brain uptake of these NET radioligands. The possibility that ketamine anaesthesia leads to an under-estimation of target- to non-target ratio also seems unlikely, since PET measurements in conscious humans in our laboratory with (*S,S*)-[C-11]MeNER did not show greater regional differentiation than in anaesthetized cynomolgus monkeys, with target- to non-target ratios of about 1.5 in both species (unpublished data).

No corrections for partial volume effects (PVE) were made in these PET measurements, since this was technically outside the scope of this study. We have observed with

[1] It should be noted that in some cases the brain uptake of some PET radioligands in non-human species may be enhanced by using P-glycoprotein modulators [25, 26]. However, this approach has not yet been developed for application in human subjects.

(*S,S*)-[C-11]MeNER and (*S,S*)-[F-18]FMeNER-D_2 that it is possible to detect specific binding to NET in the cynomolgus monkey brain, regardless of PVE correction [5, 6]. Thus, although the extent of radioactivity 'spillover' from PVE in this study is unknown, the lack of correction for PVE is considered not to compromise qualitative conclusions on the efficacy of the tested radioligands as NET probes *in vivo*.

Each of the tested radioligands was quite rapidly metabolised in cynomolgus monkey, as indicated by HPLC analysis of plasma (Fig. 4). Radioactive metabolites detected in plasma were all less lipophilic than the parent radioligand, as indicated by their shorter retention times on reverse phase HPLC. Therefore, it seems unlikely that radioactive metabolites would have significantly confounded PET images from these radioligands.

Assuming that no radiometabolites confound the PET measurements, increased target to non-target ratios might be obtained from radioligands showing either higher affinity or reduced non-specific binding or both. Lipophilicity is often considered to be a key parameter in determining both brain penetration and non-specific binding to brain tissue. Log*P* is usually taken as an index of lipophilicity for the charge-neutral version of a ligand, while Log*D* is taken as an index of lipophilicity for the sum of unionized and ionized versions of the ligand at physiological pH (7.4), which is controlled by the *pKa* values of any ionisable groups in the ligand. Hence, calculated values of Log*P*, Log*D* and pKa may be expected to have some predictive value with regard to brain entry and non-specific binding for candidate radioligands. However, consideration of these parameters for the radioligands tested in this work, along side those of previously reported NET radioligands (Fig. 1), fails to identify good correlations of these parameters with brain entry or non-specific binding.

Conclusion

The three radioligands [C-11]DMI, [C-11]talopram or [C-11]talsupram are inferior to the existing PET radioligands (e.g., (*S,S*)-[C-11]MeNER or (*S,S*)-[F-18]FMeNER-D_2) for imaging central NETs.

Acknowledgments. The authors would like to thank H. Lundbeck A/S for supplying the precursors and standards of talopram and talsupram. We are also grateful for the technical assistance of Mr. A Amir and Mr. P. Truong and the other members of the PET group at Karolinska Institutet. Mr. M Schou was supported by the Karolinska Institutet-National Institutes of Health graduate training partnership program. This work was also supported in part by the Intramural Research Program of the National Institutes of Health (National Institute of Mental Health).

References

1. Halldin C, Gulyás B, Langer O, Farde L (2001) Brain radioligands–state of the art and new trends. Q J Nucl Med 45:139–152
2. Haka MS, Kilbourn MR (1989). Synthesis and regional mouse brain distribution of [^{11}C]nisoxetine, a norepinephrine transporter inhibitor. Nucl Med Biol 16:771–774
3. Schou M, Halldin C, Sóvágó J, Pike VW, Gulyás B, Mozley PD, Johnson DP, Hall H, Innis RB, Farde L (2003) Specific *in vivo* binding to the norepinephrine transporter demonstrated with the PET radioligand, (*S,S*)-[C-11]MeNER. Nucl Med Biol 30:707–714
4. Wilson AA, Johnson DP, Mozley PD, Hussey D, Ginovart N, Nobrega J, Garcia A, Meyer J, Houle S (2003) Synthesis and *in vivo* evaluation of novel radiotracers for the *in vivo* imaging of the norepinephrine transporter. Nucl Med Biol 30:85–92
5. Ding Y-S, Lin K-S, Garza V, Carter P, Alexoff D, Logan J, Shea C, Xu Y, King P (2003). Evaluation of a new norepinephrine transporter PET ligand in baboons, both in brain and peripheral organs. Synapse 50: 345–352
6. Schou M, Halldin C, Sovago J, Pike VW, Hall H, Gulyás B, Mozley PD, Dobson D, Shchukin E, Innis RB, Farde L (2004) PET evaluation of novel radiofluorinated reboxetine analogs as norepinephrine transporter probes in the monkey brain. Synapse 53:57–67
7. Bowden CL, Schatzberg AF, Rosenbaum A, Contreras SA, Samson JA, Dessain E, Sayler M (1993) Fluoxetine and desipramine in major depressive disorder. J Clin Psychopharmacol 13:305–311
8. Bøgesø KP, Christiansen AV, Hyttel J, Liljefors T (1985) 3-Phenyl-1-indanamines. Potential antidepressant activity and potent inhibitors of dopamine, norepinephrine and serotonin uptake. J Med Chem 28: 1817–1828
9. Hyttel J (1982) Citalopram—pharmacological profile of a specific serotonin uptake inhibitor with antidepressant activity. Prog Neuro-Psychopharmacol Biol Psychiatry 6:277–295
10. Cusack B, Nelson A, Richelson E (1994) Binding of antidepressants to human brain receptors: Focus on newer generation compounds. Psychopharmacology (Berl) 114:559–565
11. Owens MJ, Morgan WN, Plott SJ, Nemeroff CB (1997) Neurotransmitter receptor and transporter binding profile of antidepressants and their metabolites. J Pharmacol Exp Ther 283:1305–1322
12. Bäckström I, Marcusson J (1990) High- and low-affinity [^{3}H]desipramine-binding sites in human postmortem brain tissue. Neuropsychobiology 23:68–73
13. Gross-Isseroff R, Israeli M, Biegon A (1988) Autoradiographic analysis of [^{3}H]desmethylimipramine binding in the human brain postmortem. Brain Res 456:120–126
14. Van Dort ME, Kim J-H, Tluczek L, Wieland DM (1997) Synthesis of ^{11}C-labeled desipramine and its metabolite 2-hydroxydesipramine: Potential radiotracers for PET studies of the norepinephrine transporter. Nucl Med Biol 24:707–711
15. McConathy J, Owens MJ, Kilts CD, Malveaux EJ, Camp VM, Votaw JR, Nemeroff CB, Goodman MM (2004) Synthesis and biological evaluation of [C-11]talopram and [C-11]talsupram: Candidate PET ligands for the norepinephrine transporter. Nucl Med Biol 31:705–718
16. Sandell J, Langer O, Larsen P, Dolle F, Vaufrey F, Demphel S, Crouzel C, Halldin C (2000) Improved specific radioactivity of the PET radioligand [C-11]FLB 457 by use of the GE medical systems PETtrace MeI MicroLab. J Labelled Compd Radiopharm 43:331–338
17. Wienhard K, Dahlbom M, Eriksson L, Michel C, Bruckbauer T, Pietrzyk U, Heiss W (1994) The ECAT Exact HR: Performance of a new high resolution positron scanner. J Comput Assist Tomogr 18:110–118
18. Karlsson P, Farde L, Halldin C, Swahn C-G, Sedvall G, Foged C, Hansen K, Skrumsager B (1993) PET examination of [C-11]NNC 687 and [C-11]NNC 756 as new radioligands for the D_1-dopamine receptor. Psychopharmacology 113:149–156
19. Charnay Y, Leger L, Vallet P, Hof P, Juovet M, Bouras C (1995) [^{3}H]Nisoxetine binding sites in the cat brain: An autoradiographic study. Neuroscience 69:259–270
20. Donnan G, Kaczmarczyk S, Paxinos G, Chilco P, Kalnins R, Woodhouse D, Mendelsohn F (1991) Distribution of catecholaminergic uptake sites in human brain as determined by quantitative [^{3}H]mazindol autoradiography. J Comp Neurol 304:419–434
21. Tejani-Butt S (1992) [^{3}H]Nisoxetine: A radioligand for quantitation of norepinephrine uptake sites by autoradiography or by homogenate binding. J Pharm Exp Ther 260:427–436
22. Halldin C, Swahn C-G, Farde L, Sedvall G (1995) Radioligand disposition and metabolism. In: Comar D, (ed) PET for Drug Development and Evaluation. Academic Publishers: Kluwer, pp. 55–65

23. Waterhouse RN (2003) Determination of lipophilicity and its use as a predictor of blood brain barrier penetration of molecular imaging agents. Mol Imaging Biol 5:376–389
24. pKa, LogD and Log P values were predicted with the Pallas 3.0 for Windows software
25. Doze P, Van Waarde A, Elsinga PH, Hendrikse NH, Vaalburg W (2000) Enhanced cerebral uptake of receptor ligands by modulation of P-glycoprotein function in the blood–brain barrier. Synapse 36:66–74
26. Balle T, Halldin C, Andersen L, Alfrangis LH, Badolo L, Jensen K.G., Chou YW, Andersen K, Perregaard J, Farde L (2004) New α_1-adrenoceptor antagonists derived from the antipsychotic sertindole—carbon-11 labelling and PET examination of brain uptake in the cynomolgus monkey. Nucl Med Biol 31:327–336
27. Hara K, Yanagihara N, Minami K, Ueno S, Toyohira Y, Sata T, Kawamura M, Bruss M, Bonisch H, Shigematsu A, Izumi F (1998) Ketamine interacts with the noradrenaline transporter at a site partly overlapping the desipramine binding site. N-S Arch Pharmacol 358:328–333
28. Uryu K, Minami K, Yanagihara N, Hara K, Toyohira Y, Izumi F, Shigematsu A (2000) Inhibition by neuromuscular blocking drugs of norepinephrine transporter in cultured bovine adrenal medullary cells. Anesth Analg 91:546–551